Current Genetics (2022) 68:143–152
https://doi.org/10.1007/s00294-021-01207-x

ORIGINAL ARTICLE

Serine–arginine protein kinase-like protein, SrpkF, stimulates both cellobiose-responsive and D-xylose-responsive signaling pathways in *Aspergillus aculeatus*

Ryohei Katayama[1] · Natsumi Kobayashi[1] · Takashi Kawaguchi[1] · Shuji Tani[1]

Received: 5 July 2021 / Revised: 12 August 2021 / Accepted: 21 August 2021 / Published online: 28 August 2021

Abstract

Aspergillus aculeatus produces cellulolytic enzymes in the presence of their substrates. We screened a library of 12,000 *A. aculeatus* T-DNA-inserted mutants to identify a regulatory factor involved in the expression of their enzyme genes in response to inducers. We found one mutant that reduced the expression of FIII-avicelase (*chbI*) in response to cellulose. T-DNA was inserted into a putative protein kinase gene similar to AN10082 in *A. nidulans*, serine–arginine protein kinase F, SrpkF. Fold increases in *srpkF* gene expression in response to various carbon sources were 2.3 (D-xylose), 44 (Avicel®), 59 (Bacto™ Tryptone), and 98 (no carbon) compared with D-glucose. Deletion of *srpkF* in *A. aculeatus* resulted in a significant reduction in cellulose-responsive expression of *chbI*, hydrocellulase (*cel7b*), and FIb-xylanase (*xynIb*) genes at an early induction phase. Further, the *srpkF*-overexpressing strain showed upregulation of the *srpkF* gene from four- to nine-fold higher than in the control strain. *srpkF* overexpression upregulated *cbhI* and *cel7b* in response to cellobiose and the FI-carboxymethyl cellulase gene (*cmc1*) and *xynIb* in response to D-xylose. However, the *srpkF* deletion did not affect the expression of *xynIb* in response to D-xylose due to the less expression of *srpkF* under the D-xylose condition. Our data demonstrate that SrpkF is primarily involved in cellulose-responsive expression, though it has a potential to stimulate gene expression in response to both cellobiose and D-xylose in *A. aculeatus*.

Keywords Gene regulation · Cellulase · ManR · XlnR · Filamentous fungi · Phosphorylation

Introduction

Lignocellulosic biomass has long been recognized as a potential sustainable source of mixed sugars for fermentation to biofuels and chemicals (Himmel et al. 2007). A key step for bioconversion of lignocellulose is enzymatic hydrolysis of pretreated lignocellulose to fermentable sugars. Filamentous fungi are prominent producers of enzymes that degrade lignocellulose (Payne et al. 2015). *Trichoderma reesei* is a well-known species that produces copious amounts of cellulolytic enzymes (Bischof et al. 2016). *T. reesei* glycoside hydrolases are being continuously improved to utilize lignocellulose as a feedstock for the generation of bio-based products. For example, *Aspergillus aculeatus* no. F-50 [NBRC 108789] was isolated from soil as a host for production of carbohydrate-active enzymes that cooperatively hydrolyze pulp in combination with *Trichoderma reesei* (Murao et al. 1979). β-Glucosidase from *A. aculeatus* no. F-50 was introduced into *T. reesei*, which accelerated cellulose hydrolysis (Baba et al. 2015; Nakazawa et al. 2012). This β-glucosidase showed high compatibility with *T. reesei*, suggesting that *A. aculeatus* produces promising enzymes for liberating fermentable sugars from lignocellulose. However, cellulolytic and xylanolytic enzymes of *A. aculeatus* are not utilized in industry because of low production levels. We aimed to understand the regulatory mechanisms of the associated genes and apply this knowledge to improving enzyme production in *A. aculeatus*.

Cellulolytic and xylanolytic enzyme production in *Aspergillus* is regulated at the transcriptional level. The first identified regulator of cellulolytic and xylanolytic genes was XlnR, a $Zn(II)_2Cys_6$-type transcriptional activator that

Communicated by Michael Polymenis.

✉ Shuji Tani
shuji@biochem.osakafu-u.ac.jp

[1] Graduate School of Life and Environmental Sciences, Osaka Prefecture University, 1-1 Gakuen-cho, Sakai, Osaka 599-8531, Japan

coordinates xylanolytic expression in *Aspergillus niger* (van Peij et al. 1998). Genetic analysis indicates that XlnR controls the expression of xylanolytic and cellulolytic enzyme genes in *A. aculeatus* (Kunitake and Kobayashi 2017; Tani et al. 2014). XlnR regulates expression of FIb-xylanase (*xynIb*) and FI-carboxymethyl cellulase (*cmc1*) genes in response to cellulose and D-xylose, respectively. In contrast, FIII-avicelase (*cbhI*), FII-carboxymethyl cellulase (*cmc2*), and *hydrocellulase* (*cel7b*) are induced in response to cellulose via an XlnR-independent signaling pathway in *A. aculeatus* (Tani et al. 2012). Clr-2 in *Neurospora crassa* and ClrB, a Clr-2 homolog in *Aspergillus nidulans,* were identified as $Zn(II)_2Cys_6$-type transcriptional activators that control expression of cellulolytic enzyme genes in response to cellulosic carbon sources (Coradetti et al. 2012). ManR, a ClrB ortholog, participates in the XlnR-independent signaling pathway in *Aspergillus oryzae* (Ogawa et al. 2013). We confirmed that ManR controls expression of *cbhI*, *cmc2*, and *cel7b* in response to cellulose, which is controlled by the XlnR-independent signaling pathway in *A. aculeatus* (Tsumura et al. 2021).

Various factors are involved in a complex regulatory network to maintain the precise balance of carbon sources required for growth and hydrolytic enzyme production. Cellodextrin transporters function as transceptors that recognize cellobiose and initiate induction of cellulase gene expression in *N. crassa* (Znameroski, et al. 2014). *Trichoderma* mitogen-activated protein kinase, Tmk2, is involved in cell wall integrity, sporulation, and cellulase production (Wang et al. 2014). Cyclic AMP-dependent protein kinase A (PKA) affects cellulase gene expression in response to light in *T. reesei* (Schuster et al. 2012). PKA in *A. nidulans* is also involved in the repression of cellulolytic enzyme genes in response to carbon sources (Kunitake et al. 2019). However, molecular mechanisms underlying cooperative control by these factors of cellulolytic and xylanolytic enzyme genes remain unknown.

We previously established a positive screening method to identify regulators involved in the cellulose-responsive induction in *A. aculeatus*. We constructed a random insertional mutagenesis library using *Agrobacterium tumefaciens*-mediated transformation of *A. aculeatus* NCP2, which harbors a transcriptional fusion between the *cbhI* promoter (P_{CBHI}) and the orotidine 5′-phosphate decarboxylase gene (*pyrG*). Cellulose-responsive expression-deficient mutants could then be isolated by screening for 5-fluoroorotic acid (5-FOA)-resistant mutants on minimal medium (MM) with wheat bran as a sole carbon source (Kunitake et al. 2011, 2013). We identified ClbR, dipeptidyl peptidase IV, and SepM as regulators that stimulate the expression of cellulolytic enzyme genes in response to cellobiose (Kunitake et al. 2015, 2013; Tani et al. 2017; Tsumura et al. 2021). ClbR is a $Zn(II)_2Cys_6$-type transcriptional activator that controls the expression of cellulolytic enzyme genes in response to cellobiose (Kunitake, et al. 2013). SepM interacts with SepL, a putative kinase in the septation initiation network complex, which participates in septa formation and regulation of ManR-dependent signaling (Tsumura et al. 2021).

We further screened for a new regulator to better understand the regulatory mechanisms underlying ManR- and XlnR-dependent signaling pathways that modulate gene expression in response to cellulose. We identified a putative protein kinase, SrpkF, which increased expression of cellulolytic and xylanolytic genes in response to cellobiose and D-xylose under control of both ManR-dependent and XlnR-dependent signaling in *A. aculeatus*.

Materials and methods

Strains, transformation, marker recycling, and T-DNA insertion

All *A. aculeatus* strains used in this study were derived from wild-type *A. aculeatus* no. F-50 [NBRC 108789]. Unless otherwise stated, all strains were propagated at 30 ℃ in an appropriately supplemented MM (Adachi et al. 2009). *A. aculeatus* NCP2 (*niaD1*::*niaD*::P_{CHB1}-*pyrG*; *pyrG1*) was used to construct *A. aculeatus* strains for T-DNA insertion via *Agrobacterium tumefaciens*-mediated transformation. Counterselection on 5-FOA and marker recycling were performed as described previously (Kunitake et al. 2011, 2013). *A. aculeatus* MR12 (*pyrG1*; Δ*ku80*) was used for the disruption and complementation of the *srpkF* gene (Tani et al. 2013). *Escherichia coli* DH5αF′ was used for plasmid construction.

Disruption and complementation of srpkF

The *A. aculeatus srpkF*-deficient mutant (*pyrG1*; Δ*ku80*; Δ*srpkF*) was created by replacing *srpkF* with the *A. nidulans* orotidine 5′-phosphate decarboxylase gene (*AnpyrG*) followed by marker recycling (Tani et al. 2013). The *srpkF* deletion cassette was constructed with the 5′ and 3′ regions of *srpkF,* which are key in homologous recombination to replace *srpkF* with *AnpyrG*) were amplified from *A. aculeatus* genomic DNA using primer pairs 2.6 k-5′srpkF/2.6 k-5′srpkR and L-kinaseF/L-kinaseR, respectively. The *AnpyrG* gene was amplified from *A. nidulans* genomic DNA using the primer pair AnpyrG-KF/AnpyrG-KR. The 3′ flanking region of *sepM* was amplified using the primer pair 2.6 k-MsrpkF/M-kinaseR to eliminate *AnpyrG* by intramolecular homologous recombination at the *srpkF* locus. The 5′ region of *AnpyrG* (responsible for marker recycling) and the 3′ region were fused via PCR using the primer pair 2.6 k-5′srpkF/L-kinaseR and subcloned

into the *Eco*RV site of pBluescriptIIKS(+) to yield pDsrpkF. The *srpkF* deletion cassette was amplified via PCR using the primer pair 2.6 k-5′srpkF/L-kinaseR from pDsrpkF and introduced into MR12 (*pyrG1*; Δ*ku80*) using the protoplast-PEG method to yield the *A. aculeatus* Δ*srpkF* plus *pyrG* strain (*pyrG1*; Δ*ku80*; Δ*srpkF*::*AnpyrG*). Marker recycling used 1×10^4 transformant spores spread onto MM supplemented with 0.01% uridine and 1 mM 5-FOA. *A. aculeatus* Δ*srpkF* (*pyrG1*; Δ*ku80*; Δ*srpkF*) was obtained by monospore isolation (Supplementary Fig. S1). Supplementary Table S1 summarizes the primers used in the study.

The *srpkF* promoter, open reading frame, and 3′-untranslated region (UTR) were first amplified using the primer pair 2.6 k-5′srpkF/M-kinaseR to complement *A. aculeatus* Δ*srpkF*. *AnpyrG* and the 3′ region required for homologous recombination at the *srpkF* locus were subsequently amplified with primer pairs AnpyrG-KF/AnpyrG-CR and C-kinaseF/C-kinaseR, respectively. The three DNA fragments were fused via PCR using the primer pair 2.6 k-5′srpkF/C-kinaseR. Finally, *A. aculeatus* Δ*srpkF* was transformed with the amplified DNA fragments to yield the *srpkF*-complemented strain (*pyrG1*; Δ*ku80*; Δ*srpkF*::*srpkF*::*AnpyrG*) (Supplementary Fig. S1).

The *A. aculeatus* SrpkF C-terminus deletion mutant was generated by introducing a stop codon at 1129 nt. The ORF with its 5′ flanking region (− 23–1,121 bp) and 3′-UTR of *srpkF* was amplified using primer pairs pK-F/srpkFstopMR-R and 3′UTRF/3′UTRR, respectively. Products were fused using PCR with primer pair pK-F/3′UTRR. The region of *AnpyrG* for marker recycling and the 3′ region required for homologous recombination at the *srpkF* locus were subsequently amplified with primer pair MRstop-srpkF-F/L-kinaseR using pDsrpkF as a template. These fragments were fused via PCR using the primer pair pK-F/L-kinaseR. Fused fragments were introduced into MR12 (Supplementary Fig. S2). *A. aculeatus* Δ*CsrpkF* (*pyrG1*; Δ*ku80*; Δ*CsrpkF*$_{1\text{-}327}$) was obtained after marker recycling. The Δ*CsrpkF* strain was complemented by the same fragments used to complement Δ*srpkF* (Supplementary Fig. S2).

The *A. aculeatus srpkF*-overexpressing strain (*pyrG1*::*Ptef-srpkF*::*AapyrG*; Δ*ku80*; Δ*srpkF*) was generated by inserting an *srpkF*-overexpressing cassette into the *A. aculeatus pyrG* locus in Δ*sprkF*. The *AapyrG* ORF with its promoter and terminator region and the *AapyrG* 3′ region were amplified using primer pairs AapyrGORFF/AapyrGORFR and AapyrG3′F/AapyrG3′R, respectively, to introduce the expression cassette at the *AapyrG* locus. The promoter region of translation elongation factor 1α gene (*Ptef*) was amplified using primer set AaPtefF/AaPtefR and subsequently fused to the *AapyrG* 3′ region via PCR using primer set AapyrG3′F/AaPtefR, followed by digestion with *Not*I and *Sac*I. The amplified *AapyrG* ORF fragment was digested with *Kpn*I and *Xba*I and subcloned into pBS *Kpn*I and *Sal*I sites. The plasmid was digested with *Not*I and *Sac*I and ligated with digested *AapyrG* 3′ and *Ptef* fragments. The *srpkF*-overexpressing cassette was amplified using primer set 5′AapyrGF/3′AapyrGR. Finally, *A. aculeatus* Δ*srpkF* was transformed with amplified DNA fragments to yield the *srpkF*-overexpressing strain (Supplementary Fig. S3).

Gene expression analysis by quantitative RT-PCR

Quantitative RT-PCR (qRT-PCR) was used to quantify the expression of cellulase and hemicellulase genes as previously described (Tani et al. 2017). 0.1% Bacto™ Tryptone (Thermo Fisher Scientific, Tokyo, Japan) was used as a neutral carbon source (noninducing condition). Indicated carbon sources were added to media supplemented with 0.1% Bacto™ Tryptone to investigate the expression of test genes. Total RNA (500 ng) was used to amplify cDNA with ReverTra Ace™ qPCR RT-Master Mix (Toyobo, Tokyo, Japan). qRT-PCR was performed in a Thermal Cycler Dice™ Real-Time System (Takara, Kyoto, Japan). For amplification, a SYBR® Green I assay using THUNDERBIRD™ SYBR® qPCR Mix (Toyobo) was performed in a 20 µl reaction. Primers used for qRT-PCR are listed in Supplementary Table S1. Expression of the glyceraldehyde-3-phosphate dehydrogenase A gene (*gpdA*) was used as an internal control. The specificity of the PCR amplification was confirmed by melting curve analysis. The expression profile of each gene was analyzed with the delta–deltaCT method. More than three biological replicates were performed for each experiment, and each replicate was evaluated in triplicate.

Additional methods

Genomic DNA preparation and Southern blotting were performed as described previously (Kunitake et al. 2013). An in-house *A. aculeatus* draft genome database was used to obtain the genomic sequence of the *srpkF* gene. Two independently amplified cDNA fragments were analyzed to determine the *srpkF* cDNA sequence. Conidia from the *A. aculeatus* strains were collected in a 0.1% Tween® 80/0.8% NaCl solution and counted using a hemocytometer. The number of conidia was normalized by colony area.

Nucleotide sequence data

Nucleotide sequence data were deposited in Japan's DNA Data Bank (DDBJ) Nucleotide Sequence Data Libraries. The accession number of *srpkF* in *A. aculeatus* is DDBJ Acc. no. LC638744.

Results

Isolation of a cellulose-responsive induction-deficient mutant from an *A. aculeatus* T-DNA insertion mutant library

We previously screened an *A. aculeatus* T-DNA insertion mutant library of approximately 12,000 transformants for strains that were 5-FOA-resistant and cellulose-responsive induction-deficient. We isolated five 5-FOA-resistant strains that showed reduced growth on medium supplemented with 1% Avicel® but showed normal growth on media supplemented with 1% glucose, 1% beechwood xylan, or 1% D-xylose (Tani et al. 2017). We further analyzed one 5-FOA-resistant strain (Q3) that showed a strong correlation between the function of the gene disrupted by T-DNA and the cellulose-responsive induction-deficient phenotype.

We first investigated *cbhI* expression profiles in response to Avicel® in Q3 because the *cbhI* promoter was fused to the *pyrG* gene. This reporter gene was used as bait to screen for factors involved in the cellulose-induced signaling pathway with the 5-FOA-resistant phenotype (Kunitake et al. 2013). Expression of *cbhI* was induced in response to Avicel® at 9 h postinduction in the control strain (NCP2) but significantly reduced in Q3 to approximately 20% of NCP2 expression levels ($p < 0.05$, Student's *t* test) (Fig. 1). Expression of *xynIb* in response to Avicel® was also significantly reduced in Q3 to approximately 30% of NCP2 expression levels ($p < 0.05$, Student's *t* test) (Fig. 1). These data suggest that the T-DNA insertion in Q3 disrupted a gene required for the induction of test genes in response to Avicel®.

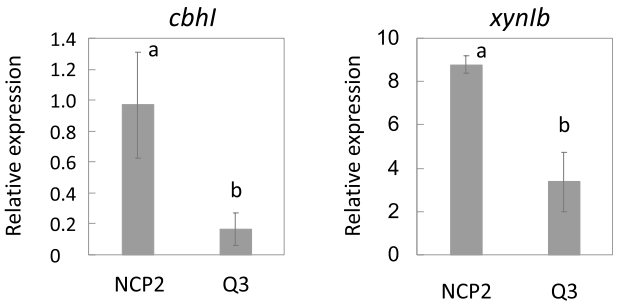

Fig. 1 Identification of a cellulose-responsive induction-deficient mutant. qRT-PCR analysis of *cbhI* and *xynIb* expression at 9 h postinduction with 1% (w/v) Avicel® was performed for control (NCP2) and Q3 strains. Relative expression corresponds to the ratio of the mean expression levels of *cbhI* divided by mean expression of *gpdA*, the reference gene. Relative expression levels are means of three independent experiments, and error bars indicate the standard deviations. Letters indicate significant differences between groups ($p < 0.05$, Student's *t* test)

Serine–arginine protein kinase F participates in the early phase of cellulose induction

T-DNA integration into Q3 was analyzed by Southern blotting since the recovery of T-DNA flanking sequences by inverse PCR differs depending on integration pattern. Genomic DNA isolated from Q3 was digested with *Eco*RI, *Xba*I and *Spe*I, *Hin*dIII, and *Pst*I. Single digestion by *Eco*RI (unique site in the T-DNA left flanking region), *Hin*dIII (absent from the vector), and *Pst*I (unique site in the vector backbone) and double digestion with *Xba*I and *Spe*I (unique site in the T-DNA right flanking region and absent from the vector, respectively) all yielded a single band (Fig. 2a). These data demonstrate that one copy of T-DNA was integrated into the Q3 genome. We amplified the T-DNA flanking sequences via inverse PCR using Q3 genomic DNA digested with *Eco*RI and *Xba*I/*Spe*I to recover the right and left flanking sequences, respectively (Fig. 2b). We sequenced DNA fragments amplified via inverse PCR, which showed that the T-DNA integrated into the ORF encoding the putative serine–threonine protein kinase (Fig. 2b). The right and left flanking sequences of the T-DNA were inserted at 1122 and 1137 nt from the translation start site of the gene with a 15 bp deletion in the recipient genome. The putative protein

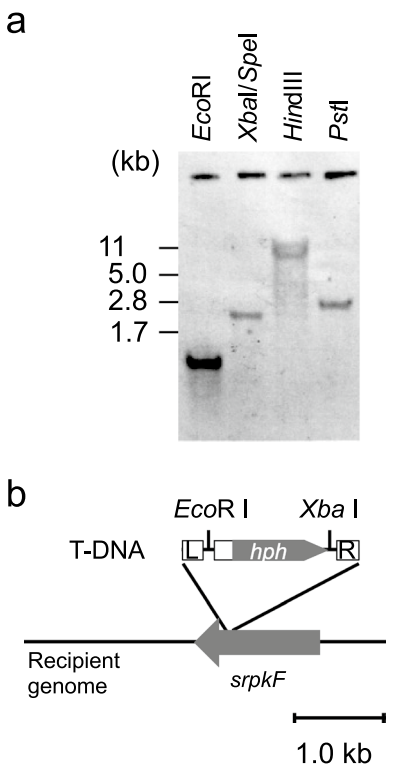

Fig. 2 Determination of the T-DNA integration pattern and identification of the disrupted gene. Deduced T-DNA integration via Southern blotting (**a**) and a schematic representation of the *SrpkF* locus (**b**)

kinase gene was composed of 1443 bp with five exons and encoded a 416-amino acid protein. Based on a homology search in FungiDB (https://fungidb.org/fungidb/), the putative protein kinase was most similar to ACLA_003920 in *Aspergillus clavatus* (*E* value = 0.0; Identities = 81%). The gene was also similar to AN10082 in *A. nidulans*, *SrpkF* (*E* value = 7e–100; Identities = 38%). This protein is a member of a family of serine–threonine protein kinases that includes an expanded group of seven serine–arginine protein kinases (SRPK) in *A. nidulans* (de Souza et al. 2013). Therefore, this gene was designated *srpkF* in *A. aculeatus*. The T-DNA insertion at 1122 nt from the translation start site caused production of a truncated protein of 327 amino acids in the original protein and seven additional amino acids (SNTDSLN) and a stop codon derived from the T-DNA fragment. Thus, *srpkF* is the candidate gene causing the cellulose-responsive induction-deficient phenotype of Q3.

The srpkF gene expressed under the carbon starvation condition

Expression profiles of *srpkF* were assessed under inducing (1% Avicel® or 1% D-xylose), repressing (1% D-glucose), carbon neutral (0.1% Bacto™ Tryptone), and carbon starvation conditions of the cellulolytic and xylanolytic enzyme genes. Transcripts of *srpkF* were quantified using RNA prepared from *A. aculeatus* wild-type strain grown under the following conditions: 1% D-glucose medium for 3 h, 1% D-xylose medium for 3 h, 1% Avicel® medium for 9 h, 0.1% Bacto™ Tryptone medium for 3 h, and no carbon source for 3 h. Fold increases in *srpkF* gene expression compared with D-glucose medium were 2.3 (D-xylose), 44 (Avicel®), 59 (Bacto™ Tryptone), and 98 (no carbon) (Fig. 3). *A. aculeatus* grew poorly in 1% Avicel® medium, 0.1% Bacto™ Tryptone medium, and under the no carbon condition, whereas it grew well on 1% glucose and 1% D-xylose media, indicating that *A. aculeatus* did not acquire sufficient carbon from 1% Avicel® and 0.1% Bacto™ Tryptone media. These data indicate that *srpkF* is expressed under conditions in which available carbon is limited.

Functional analysis of SrpkF in *A. aculeatus*

To genetically analyze the function of *srpkF*, the entire *srpkF* gene was deleted by homologous recombination (Δ*srpkF*, *pyrG*$^{+}$) followed by marker recycling to yield an *A. aculeatus srpkF* deletion mutant (Δ*srpkF*, *pyrG*$^{-}$). A *srpkF* deletion mutant was never isolated using the DNA fragment corresponding to the 1522 nt region upstream from the translation start site that was used for homologous recombination. Thus the DNA fragment from 1523 to 2613 nt upstream was targeted. Further, the 3′ flanking region of *srpkF* was deleted after marker recycling in Δ*srpkF*. Thus, the *srpkF* deletion

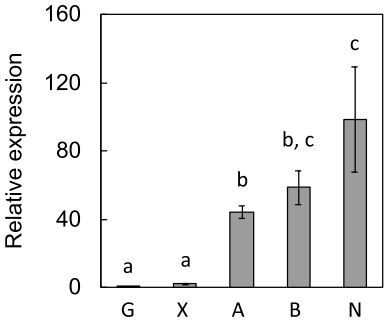

Fig. 3 qRT-PCR analysis of *srpkF* expression in wild-type *A. aculeatus* under the following conditions: 1% D-glucose for 3 h (G), 1% D-xylose for 3 h (X), 1% Avicel® for 9 h (**A**), 0.1% Bacto™ Tryptone for 3 h (**B**), and no carbon source for 3 h (N). Relative expression corresponds to the ratio of *srpkF* divided by mean expression levels of *gpdA*. Relative expression levels are means of three independent experiments, and error bars indicate the standard deviations. Letters indicate significant differences between groups ($p < 0.05$, one-way ANOVA)

mutant included elimination of 1.5 kb upstream and 1.3 kb downstream flanking sequences. Δ*srpkF* was transformed with *srpkF* DNA fragments yielding a complemented strain (*srpkF*$^{+}$) (Supplementary Fig. S1). A C-terminal deletion mutant of SrpkF composed of 327 amino acids (Δ*Csrpk*F) in Q3 was generated by introducing a stop codon at 1129 nt from the translation start site of the ORF, followed by marker recycling of *pyrG* to yield Δ*Csrpk*F (SrpkF$_{1\text{-}327}$, *pyrG*$^{-}$). Δ*Csrpk*F was also complemented using the *srpkF* DNA fragment. We confirmed that gene replacement and complementation occurred as expected by Southern blotting (Supplementary Fig. S2). MR12, Δ*srpkF*, Δ*Csrpk*F, and *srpkF*$^{+}$ grew equally well on MM supplemented with 1% D-glucose, 1% D-xylose, and 1%Avicel® (data not shown). Expression profiles of test genes in the complemented Δ*Csrpk*F strain were not different from profiles from MR12 and *srpkF*$^{+}$, and we thus used *srpkF*$^{+}$ as a control strain (data not shown).

We investigated the effect of *srpkF* deletion on gene expression in response to cellulosic carbon sources. Transcripts of *cbhI* and *xynIb* were quantified at 6 and 9 h postinduction in MR12, Δ*Csrpk*F, Δ*srpkF*, and *srpkF*$^{+}$ strains. Expression of *cbhI* and *xynIb* was reduced in Δ*Csrpk*F and Δ*srpkF* only after induction. Fold induction of *cbhI* in response to Avicel® decreased significantly to 50% in Δ*srpkF* and 31% in Δ*Csrpk*F of the response in MR12 at 9 h postinduction ($p < 0.05$, Student's *t* test). Similarly, fold induction of *xynIb* significantly decreased to 26% in Δ*srpkF* and 32% in Δ*Csrpk*F ($p < 0.05$, Student's *t* test) (Supplementary Fig. S4 and Fig. 4). SrpkF participates in the expression of both genes in response to Avicel®. Expression levels decreased similarly in both Δ*Csrpk*F and Δ*srpkF* and were restored by *srpkF* complementation. Hence, we further

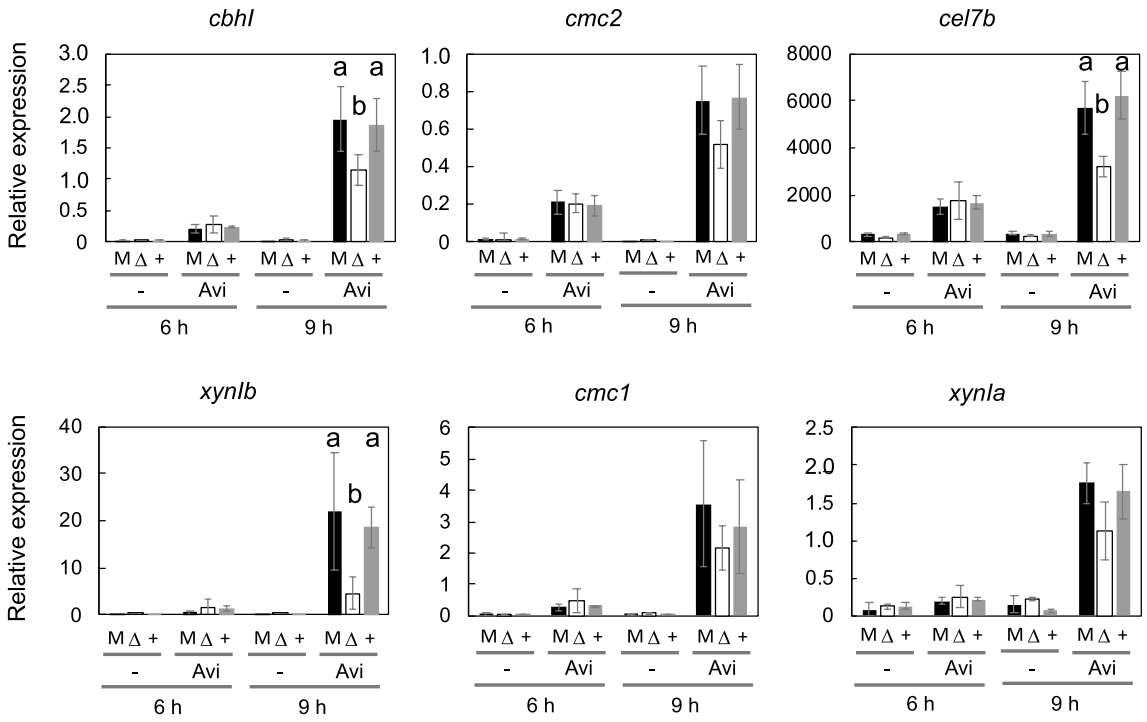

Fig. 4 Effect of *srpkF* deletion on expression of cellulase and hemicellulase genes. qRT-PCR results of each gene in MR12 (M, black bars), Δ*srpkF* (Δ, white bars), and *srpkF*$^{+}$ (+, gray bars) incubated for 6 and 9 h under the noninduced condition (−) and the 1% Avicel®-inducing condition (Avi). The relative expression corresponds to the ratio of the mean expression levels of each gene divided by that of *gpdA*. Relative expression levels are the means of three independent experiments, and the error bars indicate the standard deviations. Letters indicate significant differences between groups ($p < 0.05$, one-way ANOVA)

analyzed the SrpkF function using only Δ*srpkF*. Expression of *cel7b* in Δ*srpkF* decreased significantly to 55% of expression in MR12 at 9 h postinduction ($p < 0.05$, Student's *t* test), which was restored in *srpkF*$^{+}$ (Fig. 4). The expression of *cmc2*, *cmc1*, and *xynIa*, decreased to approximately 60%, but these reductions were not statistically significant (Fig. 4).

SrpkF participates in cellulose-responsive expression of cellulolytic and xylanolytic enzyme genes in *A. aculeatus*

To assess the effect of overexpression of *srpkF* on the expression of genes encoding cellulosic biomass-degrading enzymes in *A. aculeatus*, we constructed an *srpkF*-overexpressing strain that constitutively expresses *srpkF* under the control of the translation elongation factor 1α gene promoter (*Ptef*), a high-level constitutive promoter in *Aspergillus* (Kunitake et al. 2015). The *srpkF*-overexpressing cassette was introduced into the *pyrG* locus in Δ*srpkF* as a single copy by homologous recombination, as confirmed by Southern blotting (Supplementary Fig. S3), yielding the *srpkF*-overexpressing strain (OE*srpkF*). Expression of *srpkF* increased four to seven-fold in the presence of cellobiose with 1-deoxynojirimycin (DNJ) and approximately nine-fold in the presence of D-xylose (Supplementary Fig. S5). Since *A. aculeatus* produces β-glucosidase, which effectively hydrolyzes cellobiose to glucose, DNJ was added as a β-glucosidase inhibitor (Tani et al. 2012). The physiological phenotype of the OE*srpkF* strain was no different from MR12, ΔC*srpkF*, and Δ*srpkF* (data not shown).

We assessed the effect of *srpkF* overexpression on the expression of cellulosic biomass-degrading enzyme genes in response to physiological inducers. *cbhI*, *cmc2*, and *cel7b* were upregulated in response to cellobiose via ManR-dependent signaling. Expression of *cbhI*, *cmc2*, and *cel7b* generally increased in OE*srpkF* compared with MR12 under inducing conditions (Fig. 5a, b); however, expression profiles varied. Expression of *chbI* was induced at 2, 3, and 4 h postinduction in OE*srpkF* and resulted in a significant fold increase (Fig. 5a, b). By contrast, overexpression of *srpkF* did not significantly increase either expression or fold induction of *cmc2* (Fig. 5a, b). Expression of *cel7b* was significantly stimulated under both inducing and noninducing conditions and showed no significant difference in the fold induction. Thus, SprkF stimulated expression of *cel7b* at a basal level (Fig. 5a, b).

Expression of *xynIb* and *cmc1* is induced in response to D-xylose via XlnR-dependent signaling. Expression of *xynIb* and *cmc1* was enhanced markedly at 1.5 and 3.0 h postinduction with D-xylose in OE*srpkF* (Fig. 5c, d). These data

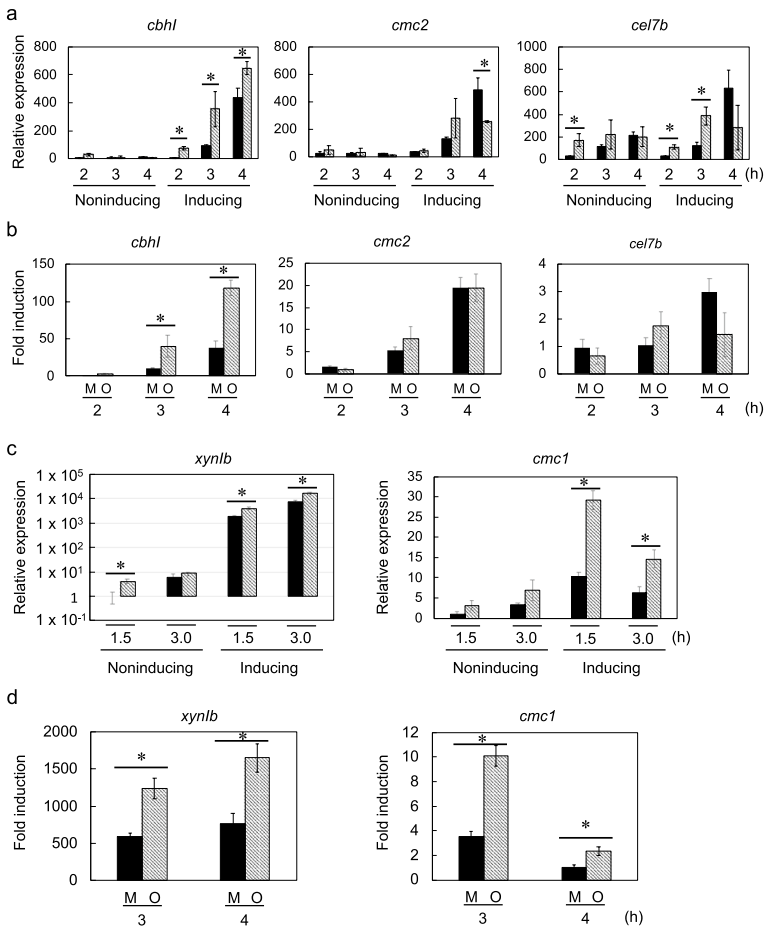

Fig. 5 Effect of *srpkF* overexpression on expression of cellulase and hemicellulase genes. qRT-PCR results for each gene in MR12 (M, black bars) and the *srpkF*-overexpressing strain OE*srpkF* (O, striped bars). **a, b** RNA was prepared from strains grown for 2–4 h in the presence of 0.1% cellobiose with 50 µg/L DNJ. Relative expression corresponds to the ratio of each gene divided by mean expression levels of *gpdA* (**a**). Fold induction of each test gene reflects the gene expression level under inducing conditions divided by expression under noninducing condition (**b**). **c**, **d** RNA was prepared from strains grown for 1.5–3.0 h in the presence of 1% (w/v) D-xylose. Relative expression corresponds to the ratio of each gene divided by mean expression levels of *gpdA* (c). **d** Fold induction of each test gene reflects gene expression under inducing conditions divided by expression under noninducing conditions (**d**). For all panels, the results shown are the means of three independent experiments, and the error bars indicate the standard deviations. An asterisk indicates a significant difference between the expression of test genes in MR12 and OE*srpkF* ($p < 0.05$, Student's *t* test)

confirm that SrpkF has a potential to participate in cellulose- and D-xylose-responsive signaling pathways.

Discussion

We identified SrpkF as a positive regulator that induces cellulolytic and xylanolytic enzyme gene expression in response to cellulose. An *srpkF*-overexpressing strain demonstrated the potential for this gene to stimulate the D-xylose-responsive induction via the XlnR-dependent signaling pathway. However, SrpkF functions as a positive regulator to stimulate cellulose-responsive induction via both ManR- and XlnR-dependent signaling under physiological conditions. *srpkF* expression was stimulated under cellulose and carbon starvation condition but not by the presence of D-xylose (Fig. 6).

A comparison of amino acid sequences using the FASTA algorithm indicated that *srpkF* orthologs are highly conserved in the *Aspergillus* section *Nigri*. Orthologs are also present in some strains from other sections and other genera, such as *A. nidulans* (AN10082, *E* value = 2e-91; Identities = 42%), *Penicillium rubens* (Pc12g16110, *E* value = 1e-104; Identities = 47%), and *Coccidioides immitis* (CIMG_04484, *E* value = 6e-103; Identities = 44%) (Fig. 7). AN10082 in *A. nidulans* encodes a serine–arginine protein kinase F (SrpkF) for which a deletion mutant did not show a distinguishing phenotype (de Souza et al. 2013). SRPK was first identified as a cell cycle-regulated kinase specific for SR proteins, which are a family of pre-mRNA splicing factors

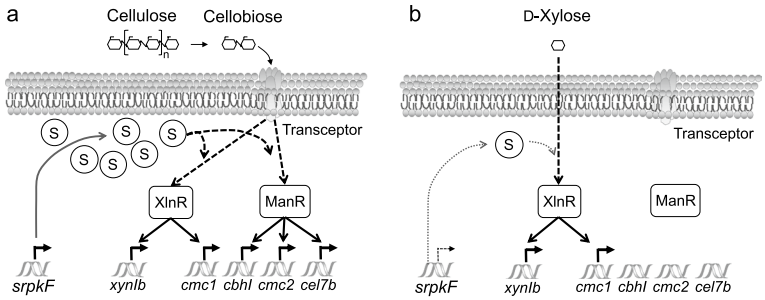

Fig. 6 Schematic illustration of possible mechanisms for SrpkF induction of cellulolytic and xylanolytic enzyme genes in *A. aculeatus*. *S* SrpkF protein

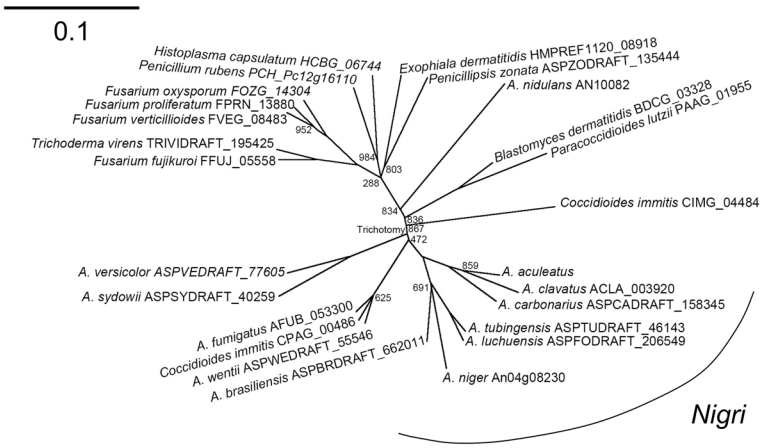

Fig. 7 Phylogenetic analysis of serine–arginine protein kinase-like genes. Phylogenetic relationships among *srpk* orthologs are shown as a consensus neighbor-joining tree based on sequences orthologous to *srpkF* in *A. aculeatus*. Alignment used ClustalW. Individual nodes were examined with 1000 bootstrap replicates; only values below 1000 are shown

containing SR domains that consist largely of serine/arginine repeats (Gui et al. 1994a, b). Members of this kinase family are known to phosphorylate serines within SR domains and are widely conserved in eukaryotes. *S. cerevisiae* encodes a single SRPK family member, Sky1, but *A. nidulans* and *A. aculeatus* encode seven SRPKs from SrpkA to G (de Souza et al. 2013) and four SRPKs, respectively. SrpkA proteins in *Aspergillus* are highly conserved along with *S. cerevisiae* Sky1. Thus, these proteins may modulate subcellular localization and function of Ser-Arg rich splicing-factor proteins (Dagher and Fu 2001; Gui et al. 1994a). However, SRPKs possess various domains, suggesting functional diversification. Few non-splicing functions of SRPKs are reported (Gou et al. 2020; Hong et al. 2012; Wang et al. 2017), and it remains unclear whether SRPKs have evolved further regulatory roles (Bustos et al. 2020). Functions of SRPKs might be illuminated by close examination of gene expression since some genes exhibited highly tissue-specific profiles (Nakagawa et al. 2005; Wang et al. 1998).

The expression of *srpkF* increased under carbon-limited conditions, such as the no carbon and Avicel® conditions (Fig. 3), which showed strong correlations between SrpkF functions in cellulose-responsive induction and expression profiles. We focused on two signaling pathways involved in cellulose-responsive induction in *A. aculeatus* to narrow possible pathways. One is ManR-dependent signaling that induces expression of *cbhI*, *cmc2*, and *cel7b*. We expected that deletion and overexpression of *srpkF* would show a consistent effect on these three genes. However, effects varied, suggesting that transcription factors other than ManR could be involved. Overexpression of *clbR*, a putative transcription factor involved in cellobiose-responsive induction in *A. aculeatus*, did not affect the expression of *cbhI* and *cmc2* but did reduce the expression of *cel7b*. Still, deletion of *clbR* reduced their expression levels in response to Avicel® (Kunitake et al. 2015). These data suggest that various factors participate in ManR-dependent signaling in response to cellulosic carbon sources in *A. aculeatus*.

Interestingly, overexpression of *srpkF* promoted xylanase gene expression in response to D-xylose, but no effect of *srpkF* deletion was seen for xylose-responsive expression of the xylanase gene. SrpkF is thus critically regulated at the transcription level. How SrpkF participates in the two different signaling pathways in response to cellulose and D-xylose is not clear. XlnR is constitutively expressed in *A. oryzae* and is phosphorylated in the presence of D-xylose then rapidly dephosphorylated by removing D-xylose from the medium (Noguchi et al. 2011). ManR phosphorylation status is unknown and SrpkF is a candidate kinase that could be involved in ManR- and XlnR-dependent signaling (Fig. 6).

A recent study addressed levels of conservation and diversity in the regulatory mechanisms of cellulolytic enzyme genes in Ascomycete fungi (Kunitake and Kobayashi 2017). XlnR controls the transcription of 20–30 genes encoding

cellulolytic and xylanolytic enzymes in the presence of cellulose in *A. niger* (Stricker et al. 2008). XlnR mainly regulates the expression of xylanolytic enzyme genes for *A. oryzae* and *A. aculeatus* and is only marginally involved in the expression of cellulolytic enzyme genes in response to cellulose (Marui et al. 2002; Tani et al. 2012). In contrast, Xyr1, an XlnR ortholog in *T. reesei*, is a master regulator that modulates the expression of xylanolytic and cellulolytic enzyme genes in response to various carbon sources, such as D-xylose, sophorose, galactose, and lactose (Stricker et al. 2006, 2007). XLR-1 in *N. crassa* participates in the induction of xylanolytic but not significantly involved in the induction of cellulolytic enzyme genes (Sun et al. 2012). The expression of cellulolytic enzyme genes is mainly regulated by ManR in *A. oryzae* and *A. aculeatus* (Ogawa et al. 2013; Tsumura et al. 2021) and its orthologs ClrB in *A. nidulans* and CLR-2 in *N. crassa* (Coradetti et al. 2012, 2013). Complex regulation mechanisms can be conferred by the acquisition of paralogous genes that establish new signal transduction pathways (Baker et al. 2013). Orthologous genes of *srpkF* are absent from the genomes of several cellulase-producing fungi, such as *Trichoderma* and *Neurospora* species. The acquisition of *srpkF* in *Aspergillus* might lead to differential regulation of cellulolytic enzyme genes. A logical next step is to identify target proteins of SrpkF, which will help understand the complex regulatory mechanisms of cellulolytic enzyme genes in *Aspergillus*.

Supplementary Information The online version contains supplementary material available at https://doi.org/10.1007/s00294-021-01207-x.

Acknowledgements This work was supported by Grants-in-Aid for Scientific Research from the Japan Society for the Promotion of Science under Grant 19K05777. Part of this work was also supported by the New Energy and Industrial Technology Development Organization Project under Grant P07015.

Author's contributions S.T. and T.K. conceived and designed the project. R.K. and N.K. conducted the experiments. S.T wrote the paper. All authors read and approved the final manuscript.

Funding This work was supported by JSPS KAKENHI under Grant 19K05777. Part of this work was also supported by the New Energy and Industrial Technology Development Organization (NEDO) Project under Grant P07015.

Declarations

Conflict of interest The authors have no conflicts of interest to declare that are relevant to the content of this article.

Ethical approval This article does not contain any studies that involve human participants or animals.

Consent to participate Not applicable.

Consent for publication Not applicable.

Data availability All data generated or analyzed during this study are included in this published article and its Supplementary Information files. DNA sequences will be available at the DDBJ database when this article is released for publication.

Code availability Not applicable.

References

Adachi H, Tani S, Kanamasa S, Sumitani J, Kawaguchi T (2009) Development of a homologous transformation system for *Aspergillus aculeatus* based on the *sC* gene encoding ATP-sulfurylase. Biosci Biotechnol Biochem 73:1197–1199. https://doi.org/10.1271/bbb.80772

Baba Y, Sumitani J, Tani S, Kawaguchi T (2015) Characterization of *Aspergillus aculeatus* β-glucosidase 1 accelerating cellulose hydrolysis with *Trichoderma* cellulase system. AMB Express 5:3. https://doi.org/10.1186/s13568-014-0090-3

Baker CR, Hanson-Smith V, Johnson AD (2013) Following gene duplication, paralog interference constrains transcriptional circuit evolution. Science 342:104–108. https://doi.org/10.1126/science.1240810

Bischof RH, Ramoni J, Seiboth B (2016) Cellulases and beyond: the first 70 years of the enzyme producer *Trichoderma reesei*. Microb Cell Fact 15:106. https://doi.org/10.1186/s12934-016-0507-6

Bustos F, Segarra-Fas A, Nardocci G, Cassidy A, Antico O, Davidson L, Brandenburg L, Macartney TJ, Toth R, Hastie CJ, Moran J, Gourlay R, Varghese J, Soares RF, Montecino M, Findlay GM (2020) Functional diversification of SRSF protein kinase to control ubiquitin-dependent neurodevelopmental signaling. Dev Cell 55(629–647):e627. https://doi.org/10.1016/j.devcel.2020.09.025

Coradetti S, Craig J, Xiong Y, Shock T, Tian C, Glass N (2012) Conserved and essential transcription factors for cellulase gene expression in Ascomycete fungi. Proc Natl Acad Sci USA 109:7397–7402. https://doi.org/10.1073/pnas.1200785109

Coradetti ST, Xiong Y, Glass NL (2013) Analysis of a conserved cellulase transcriptional regulator reveals inducer-independent production of cellulolytic enzymes in *Neurospora crassa*. MicrobiologyOpen 2:595–609. https://doi.org/10.1002/mbo3.94

Dagher SF, Fu XD (2001) Evidence for a role of Sky1p-mediated phosphorylation in 3' splice site recognition involving both Prp8 and Prp17/Slu4. RNA 7:1284–1297. https://doi.org/10.1017/s1355838201016077

de Souza CP, Hashmi SB, Osmani AH, Andrews P, Ringelberg CS, Dunlap JC, Osmani SA (2013) Functional analysis of the *Aspergillus nidulans* kinome. PLoS One 8:e58008. https://doi.org/10.1371/journal.pone.0058008

Gui JF, Chandler SD, Fu XD (1994a) Purification and characterization of a kinase specific for the serine- and arginine-rich pre-mRNA splicing factors. Proc Natl Acad Sci U S A 91:10824–10828. https://doi.org/10.1073/pnas.91.23.10824

Gui JF, Lane WS, Fu XD (1994b) A serine kinase regulates intracellular localization of splicing factors in the cell cycle. Nature 1994:678–682. https://doi.org/10.1038/369678a0

Gou LT, Lim DH, Ma W, Aubol BE, Hao Y, Wang X, Zhao J, Liang Z, Shao C, Zhang X et al (2020) Initiation of parental genome reprogramming in fertilized oocyte by splicing kinase SRPK1-catalyzed protamine phosphorylation. Cell 180:1212–1227, e1214. https://doi.org/10.1016/j.cell.2020.02.020

Himmel ME, Ding SY, Johnson DK, Adney WS, Nimlos MR, Brady JW, Foust TD (2007) Biomass recalcitrance: engineering plants and enzymes for biofuels production. Science 315:804–807. https://doi.org/10.1126/science.1137016

Hong Y, Chan CB, Kwon IS, Li X, Song M, Lee HP, Liu X, Sompol P, Jin P, Lee HG, Yu SP, Ye K (2012) SRPK2 phosphorylates tau and mediates the cognitive defects in Alzheimer's disease. J Neurosci 32:17262–17272. https://doi.org/10.1523/JNEUROSCI.3300-12.2012

Kunitake E, Kobayashi T (2017) Conservation and diversity of the regulators of cellulolytic enzyme genes in ascomycete fungi. Curr Genet 63:951–958. https://doi.org/10.1007/s00294-017-0695-6

Kunitake E, Tani S, Sumitani J, Kawaguchi T (2011) *Agrobacterium tumefaciens*-mediated transformation of *Aspergillus aculeatus* for insertional mutagenesis. AMB Express 1:46. https://doi.org/10.1186/2191-0855-1-46

Kunitake E, Tani S, Sumitani J, Kawaguchi T (2013) A novel transcriptional regulator, ClbR, controls the cellobiose- and cellulose-responsive induction of cellulase and xylanase genes regulated by two distinct signaling pathways in *Aspergillus aculeatus*. Appl Microbiol Biotechnol 97:2017–2028. https://doi.org/10.1007/s00253-012-4305-8

Kunitake E, Kawamura A, Tani S, Takenaka S, Ogasawara W, Sumitani J, Kawaguchi T (2015) Effects of *clbR* overexpression on enzyme production in *Aspergillus aculeatus* vary depending on the cellulosic biomass-degrading enzyme species. Biosci Biotechnol Biochem 79:488–495. https://doi.org/10.1080/09168451.2014.982501

Kunitake E, Li Y, Uchida R, Nohara T, Asano K, Hattori A, Kimura T, Kanamaru K, Kimura M, Kobayashi T (2019) CreA-independent carbon catabolite repression of cellulase genes by trimeric G-protein and protein kinase A in *Aspergillus nidulans*. Curr Genet 65:941–952. https://doi.org/10.1007/s00294-019-00944-4

Marui J, Kitamoto N, Kato M, Kobayashi T, Tsukagoshi N (2002) Transcriptional activator, AoXlnR, mediates cellulose-inductive expression of the xylanolytic and cellulolytic genes in *Aspergillus oryzae*. FEBS Lett 528:279–282. https://doi.org/10.1016/s0014-5793(02)03328-8

Murao S, Kanamoto J, Arai M (1979) Isolation and identification of a cellulolytic enzyme producing microorganism. J Ferment Technol 57:151–156

Nakagawa O, Arnold M, Nakagawa M, Hamada H, Shelton JM, Kusano H, Harris TM, Childs G, Campbell KP, Richardson JA, Nishino I, Olson EN (2005) Centronuclear myopathy in mice lacking a novel muscle-specific protein kinase transcriptionally regulated by MEF2. Genes Dev 19:2066–2077. https://doi.org/10.1101/gad.1338705

Nakazawa H, Kawai T, Ida N, Shida Y, Kobayashi Y, Okada H, Tani S, Sumitani J, Kawaguchi T, Morikawa Y, Ogasawara W (2012) Construction of a recombinant *Trichoderma reesei* strain expressing *Aspergillus aculeatus* β-glucosidase 1 for efficient biomass conversion. Biotechnol Bioeng 109:92–99. https://doi.org/10.1002/bit.23296

Noguchi Y, Tanaka H, Kanamaru K, Kato M, Kobayashi T (2011) Xylose triggers reversible phosphorylation of XlnR, the fungal transcriptional activator of xylanolytic and cellulolytic genes in *Aspergillus oryzae*. Biosci Biotechnol Biochem 75:953–959. https://doi.org/10.1271/bbb.100923

Ogawa M, Kobayashi T, Koyama Y (2013) ManR, a transcriptional regulator of the β-mannan utilization system, controls the cellulose utilization system in *Aspergillus oryzae*. Biosci Biotechnol Biochem 77:426–429. https://doi.org/10.1271/bbb.120795

Payne CM, Knott BC, Mayes HB, Hansson H, Himmel ME, Sandgren M, Ståhlberg J, Beckham GT (2015) Fungal cellulases. Chem Rev 115:1308–1448. https://doi.org/10.1021/cr500351c

Schuster A, Tisch D, Seidl-Seiboth V, Kubicek CP, Schmoll M (2012) Roles of protein kinase A and adenylate cyclase in light-modulated cellulase regulation in *Trichoderma reesei*. Appl Environ Microbiol 78:2168–2178. https://doi.org/10.1128/AEM.06959-11

Stricker AR, Grosstessner-Hain K, Würleitner E, Mach RL (2006) Xyr1 (xylanase regulator 1) regulates both the hydrolytic enzyme system and D-xylose metabolism in *Hypocrea jecorina*. Eukaryot Cell 5:2128–2137. https://doi.org/10.1128/ec.00211-06

Stricker AR, Steiger MG, Mach RL (2007) Xyr1 receives the lactose induction signal and regulates lactose metabolism in *Hypocrea jecorina*. FEBS Lett 581:3915–3920. https://doi.org/10.1016/j.febslet.2007.07.025

Stricker AR, Mach RL, de Graaff LH (2008) Regulation of transcription of cellulases- and hemicellulases-encoding genes in *Aspergillus niger* and *Hypocrea jecorina* (*Trichoderma reesei*). Appl Microbiol Biotechnol 78:211–220. https://doi.org/10.1007/s00253-007-1322-0

Sun J, Tian C, Diamond S, Glass NL (2012) Deciphering transcriptional regulatory mechanisms associated with hemicellulose degradation in *Neurospora crassa*. Eukaryot Cell 11:482–493. https://doi.org/10.1128/EC.05327-11

Tani S, Kanamasa S, Sumitani J, Arai M, Kawaguchi T (2012) XlnR-independent signaling pathway regulates both cellulase and xylanase genes in response to cellobiose in *Aspergillus aculeatus*. Curr Genet 58:93–104. https://doi.org/10.1007/s00294-012-0367-5

Tani S, Tsuji A, Kunitake E, Sumitani J, Kawaguchi T (2013) Reversible impairment of the *ku80* gene by a recyclable marker in *Aspergillus aculeatus*. AMB Express 3:4. https://doi.org/10.1186/2191-0855-3-4

Tani S, Kawaguchi T, Kobayashi T (2014) Complex regulation of hydrolytic enzyme genes for cellulosic biomass degradation in filamentous fungi. Appl Microbiol Biotechnol 98:4829–4837. https://doi.org/10.1007/s00253-014-5707-6

Tani S, Yuki S, Kunitake E, Sumitani J, Kawaguchi T (2017) Dipeptidyl peptidase IV is involved in the cellulose-responsive induction of cellulose biomass-degrading enzyme genes in *Aspergillus aculeatus*. Biosci Biotechnol Biochem 81:1227–1234. https://doi.org/10.1080/09168451.2017.1295800

Tsumura R, Sawada K, Kunitake E, Sumitani J, Kawaguchi T, Tani S (2021) A component of the septation initiation network complex, AaSepM, is involved in multiple cellulose-responsive signaling pathways in *Aspergillus aculeatus*. Appl Microbiol Biotechnol 105:1535–1546. https://doi.org/10.1007/s00253-021-11110-7

van Peij NN, Visser J, de Graaff LH (1998) Isolation and analysis of XlnR, encoding a transcriptional activator co-ordinating xylanolytic expression in *Aspergillus niger*. Mol Microbiol 27:131–142. https://doi.org/10.1046/j.1365-2958.1998.00666.x

Wang HY, Lin W, Dyck JA, Yeakley JM, Songyang Z, Cantley LC, Fu XD (1998) SRPK2: A differentially expressed SR protein-specific kinase involved in mediating the interaction and localization of pre-mRNA splicing factors in mammalian cells. J Cell Biol 140:737–750. https://doi.org/10.1083/jcb.140.4.737

Wang M, Dong Y, Zhao Q, Wang F, Liu K, Jiang B, Fang X (2014) Identification of the role of a MAP kinase Tmk2 in *Hypocrea jecorina* (*Trichoderma reesei*). Sci Rep 4:6732. https://doi.org/10.1038/srep06732

Wang ZH, Liu P, Liu X, Manfredsson FP, Sandoval IM, Yu SP, Wang JZ, Ye K (2017)Delta-secretase phosphorylation by SRPK2 enhances its enzymatic activity, provoking pathogenesis in Alzheimer's disease. Mol cell 67:812–825, e815. https://doi.org/10.1016/j.molcel.2017.07.018

Znameroski EA, Li X, Tsai JC, Galazka JM, Glass NL, Cate JH (2014) Evidence for transceptor function of cellodextrin transporters in *Neurospora crassa*. J Biol Chem 289:2610–2619. https://doi.org/10.1074/jbc.M113.533273